

# Scalar neutrino dark matter in $U(1)_X$ SSM

Shu-Min Zhao<sup>1\*</sup>, Tai-Fu Feng<sup>1†</sup>, Ming-Jie Zhang<sup>1</sup>,

Jin-Lei Yang<sup>1</sup>, Hai-Bin Zhang<sup>1</sup>, Guo-Zhu Ning<sup>1</sup>

<sup>1</sup> *Department of Physics, Hebei University, Baoding 071002, China*

(Dated: May 29, 2019)

## Abstract

$U(1)_X$ SSM is the extension of the minimal supersymmetric standard model(MSSM) and its local gauge group is  $SU(3)_C \times SU(2)_L \times U(1)_Y \times U(1)_X$ . Compared with MSSM, it has three singlet new Higgs superfields and right handed neutrinos. In the framework of  $U(1)_X$ SSM, we study the Higgs mass and suppose the lightest CP-even sneutrino as cold dark matter candidate. For the lightest CP-even sneutrino, the relic density and the cross section with nucleon are both researched. In our chosen parameter space, the numerical results show that considering the lightest CP-even sneutrino as cold dark matter the obtained results satisfy the constraints from the relic density and the scattering off nucleon.

PACS numbers:

Keywords: dark matter, sneutrino, supersymmetry

---

\* zhaosm@hbu.edu.cn

† fengtf@hbu.edu.cn

## I. INTRODUCTION

From the cosmological observations, astronomers are sure of the existence of dark matter in the universe, where the dark matter is about five times that of visible matter contribution[1]. The various luminous objects (stars, gas clouds globular clusters or entire galaxies) move faster than one expects[2]. These observations are the earliest and most convincing evidence for dark matter[3, 4]. Dark matter must be electrically and color neutral, and can only take part in weak interactions. To have a long life, it should be stable[5]. Up to now, people have not known the mass and interaction properties of the dark matter.

Though the standard model achieves great success with detection of the CP-even Higgs(125.1GeV)[6], it can not explain the relic density of dark matter in the universe. The relic density of light neutrinos with tiny mass is  $\Omega_\nu h^2 \leq 0.0062$  at 95% confidence level, that is much smaller than non-baryonic matter density  $\Omega_\nu h^2 = 0.1186 \pm 0.0020$ [7]. So there must exist new physics beyond the standard model! There are several dark matter candidates: axions, sterile neutrinos, primordial black holes and weakly interacting massive particles(WIMPs)[8]. WIMP is one of the most popular candidates for dark matter, whose detection is crucial for both distinguishing new physics models and understanding the nature of dark matter. The direct detection for dark matter is to study the recoil energy of nuclei caused by the elastic scattering of a WIMP off a nucleon.

As one of the favorite dark matter candidate, the neutralino in the minimal supersymmetric standard model(MSSM) has been extensively studied[9]. However, the left-handed sneutrino meets severe troubles, because the cross section for elastic scattering off nuclei exceeds the experimental limit about several orders with the exchange of vector boson Z[10]. Considering the neutrino oscillations, we find that neutrino should possess tiny mass[11]. In order to obtain light neutrino mass, one can add right-handed neutrino to the MSSM. The supersymmetric partners of the right-handed neutrinos will produce an alternative dark matter candidate[12]. The sneutrino dark matter are researched in the extension of NMSSM by the authors[13], and there are also other works of sneutrino dark matter [14, 15].

In this work, we extend MSSM to  $U(1)_X$ SSM, whose local gauge group is  $SU(3)_C \times SU(2)_L \times U(1)_Y \times U(1)_X$  [16]. Comparing with MSSM,  $U(1)_X$ SSM has more superfields: right-handed neutrinos and three  $SU(2)_L$  singlet Higgs superfields  $\hat{\eta}$ ,  $\hat{\bar{\eta}}$ ,  $\hat{S}$ . The right-handed neutrinos can produce tiny masses to light neutrinos through see-saw mechanism. The little

hierarchy problem in MSSM is relieved in  $U(1)_X$ SSM by the right-handed neutrinos and sneutrinos. The added parameters mitigate the constraints from experiments such as LHC. Comparing with MSSM, there are more dark matter candidates in the  $U(1)_X$ SSM.

After this introduction, we introduce the  $U(1)_X$ SSM in detail in section II. Supposing the lightest CP-even sneutrino as dark matter candidate, we study its relic density in section III. Section IV is used to research the direct detection for sneutrino in the nuclei. The numerical results for Higgs masses, relic density for dark matter and its direct detection are all collected in section V. In section VI, we show our discussion and conclusion.

## II. THE $U(1)_X$ SSM

The local gauge group of the  $U(1)_X$ SSM is  $SU(3)_C \otimes SU(2)_L \otimes U(1)_Y \otimes U(1)_X$ . To obtain  $U(1)_X$ SSM more superfields: right-handed neutrino  $\hat{\nu}_i$  and three Higgs singlets  $\hat{\eta}$ ,  $\hat{\bar{\eta}}$ ,  $\hat{S}$  are added to MSSM. It can give light neutrino mass at tree level through see-saw mechanism. The neutral CP-even parts of  $H_u$ ,  $H_d$ ,  $\eta$ ,  $\bar{\eta}$ ,  $S$  mix together and form  $5 \times 5$  mass squared matrix. It is interesting that, the lightest mass eigenstate of this matrix can even reach 125 GeV at tree level. However, in the MSSM and its some extended models, the lightest CP-even Higgs mass is no more than 90 GeV at tree level, so to obtain 125 GeV Higgs mass, the loop corrections are very important and depend on the virtual particle masses in the loop.

Here we show the superpotential in this model

$$W = l_W \hat{S} + \mu \hat{H}_u \hat{H}_d + M_S \hat{S} \hat{S} - Y_d \hat{d} \hat{q} \hat{H}_d - Y_e \hat{e} \hat{l} \hat{H}_d + \lambda_H \hat{S} \hat{H}_u \hat{H}_d + \lambda_C \hat{S} \hat{\eta} \hat{\bar{\eta}} + \frac{\kappa}{3} \hat{S} \hat{S} \hat{S} + Y_u \hat{u} \hat{q} \hat{H}_u + Y_X \hat{\nu} \hat{\eta} \hat{\bar{\nu}} + Y_\nu \hat{\nu} \hat{l} \hat{H}_u. \quad (1)$$

There are two Higgs doublets and three Higgs singlets, whose concrete forms are shown in the follow,

$$\begin{aligned} H_u &= \begin{pmatrix} H_u^+ \\ \frac{1}{\sqrt{2}}(v_u + H_u^0 + iP_u^0) \end{pmatrix}, & H_d &= \begin{pmatrix} \frac{1}{\sqrt{2}}(v_d + H_d^0 + iP_d^0) \\ H_d^- \end{pmatrix}, \\ \eta &= \frac{1}{\sqrt{2}}(v_\eta + \phi_\eta^0 + iP_\eta^0), & \bar{\eta} &= \frac{1}{\sqrt{2}}(v_{\bar{\eta}} + \phi_{\bar{\eta}}^0 + iP_{\bar{\eta}}^0), \\ S &= \frac{1}{\sqrt{2}}(v_S + \phi_S^0 + iP_S^0). \end{aligned} \quad (2)$$

TABLE I: The superfields in  $U(1)_X$ SSM

Superfields	$SU(3)_C$	$SU(2)_L$	$U(1)_Y$	$U(1)_X$
$\hat{Q}_i$	3	2	1/6	0
$\hat{u}_i^c$	$\bar{3}$	1	-2/3	-1/2
$\hat{d}_i^c$	$\bar{3}$	1	1/3	1/2
$\hat{L}_i$	1	2	-1/2	0
$\hat{e}_i^c$	1	1	1	1/2
$\hat{\nu}_i$	1	1	0	-1/2
$\hat{H}_u$	1	2	1/2	1/2
$\hat{H}_d$	1	2	-1/2	-1/2
$\hat{\eta}$	1	1	0	-1
$\hat{\bar{\eta}}$	1	1	0	1
$\hat{S}$	1	1	0	0

$v_u$ ,  $v_d$ ,  $v_\eta$ ,  $v_{\bar{\eta}}$  and  $v_S$  are the corresponding vacuum expectation values (VEVs) of the Higgs fields  $H_u$ ,  $H_d$ ,  $\eta$ ,  $\bar{\eta}$  and  $S$ . Here, we define  $\tan \beta = v_u/v_d$  and  $\tan \beta_\eta = v_{\bar{\eta}}/v_\eta$ . The definition of  $\tilde{\nu}_L(\tilde{\nu}_R)$  is

$$\tilde{\nu}_L = \frac{1}{\sqrt{2}}\phi_l + \frac{i}{\sqrt{2}}\sigma_l, \quad \tilde{\nu}_R = \frac{1}{\sqrt{2}}\phi_R + \frac{i}{\sqrt{2}}\sigma_R. \quad (3)$$

The soft breaking terms are

$$\begin{aligned} \mathcal{L}_{soft} = & \mathcal{L}_{soft}^{MSSM} - B_S S^2 - L_S S - \frac{T_\kappa}{3} S^3 - T_{\lambda_C} S \eta \bar{\eta} + \epsilon_{ij} T_{\lambda_H} S H_d^i H_u^j \\ & - T_X^{IJ} \bar{\eta} \tilde{\nu}_R^{*I} \tilde{\nu}_R^{*J} + \epsilon_{ij} T_\nu^{IJ} H_u^i \tilde{\nu}_R^{*I} \tilde{l}_j^J - m_\eta^2 |\eta|^2 - m_{\bar{\eta}}^2 |\bar{\eta}|^2 \\ & - m_S^2 S^2 - (m_{\tilde{\nu}_R}^2)^{IJ} \tilde{\nu}_R^{*I} \tilde{\nu}_R^J - \frac{1}{2} (M_X \lambda_{\tilde{X}}^2 + 2 M_{BB'} \lambda_{\tilde{B}} \lambda_{\tilde{X}}) + h.c. \quad . \end{aligned} \quad (4)$$

The presence of two Abelian groups  $U_Y(1)$  and  $U_X(1)$  in  $U_X(1)$ SSM has a new effect absent in the MSSM with just one Abelian gauge group  $U_Y(1)$ : the gauge kinetic mixing. This effect can also be induced through RGEs, even if it is set to zero at  $M_{GUT}$ .

The covariant derivatives of this model is shown in the general form [17]

$$D_\mu = \partial_\mu - i \begin{pmatrix} Y & X \end{pmatrix} \begin{pmatrix} g_Y & g'_{YX} \\ g'_{XY} & g'_X \end{pmatrix} \begin{pmatrix} A_\mu^Y \\ A_\mu^X \end{pmatrix}. \quad (5)$$

Here  $A_\mu^Y$  and  $A_\mu^X$  denote the gauge fields of  $U(1)_Y$  and  $U(1)_X$ , while  $Y$  and  $X$  represent the hypercharge and  $X$  charge respectively. We can perform a change of the basis, because the two Abelian gauge groups are unbroken. The following formula can be obtained with a correct matrix  $R$  [18]

$$\begin{pmatrix} g_Y & g'_{YX} \\ g'_{XY} & g'_X \end{pmatrix} R^T = \begin{pmatrix} g_1 & g_{YX} \\ 0 & g_X \end{pmatrix}. \quad (6)$$

So the  $U(1)$  gauge fields are redefined as

$$R \begin{pmatrix} A_\mu^Y \\ A_\mu^X \end{pmatrix} = \begin{pmatrix} A_\mu^Y \\ A_\mu^X \end{pmatrix}. \quad (7)$$

The interesting thing is that the bosons  $A^X$ ,  $A^Y$  and  $V^3$  mix together at the tree level, and the mass matrix is shown in the basis  $(A^Y, V^3, A^X)$

$$\begin{pmatrix} \frac{1}{8}g_1^2v^2 & -\frac{1}{8}g_1g_2v^2 & \frac{1}{8}g_1g_{YX}v^2 \\ -\frac{1}{8}g_1g_2v^2 & \frac{1}{8}g_2^2v^2 & -\frac{1}{8}g_2g_{YX}v^2 \\ \frac{1}{8}g_1g_{YX}v^2 & -\frac{1}{8}g_2g_{YX}v^2 & \frac{1}{8}g_{YX}^2v^2 + \frac{1}{8}g_X^2\xi^2 \end{pmatrix}. \quad (8)$$

with  $v^2 = v_u^2 + v_d^2$  and  $\xi^2 = v_\eta^2 + v_{\bar{\eta}}^2$ . To diagonalize the mass matrix in Eq.(8), an unitary matrix including two mixing angles  $\theta_W$  and  $\theta'_W$  is used here

$$\begin{pmatrix} \gamma \\ Z \\ Z' \end{pmatrix} = \begin{pmatrix} \cos \theta_W & \sin \theta_W & 0 \\ -\sin \theta_W \cos \theta'_W & \cos \theta_W \cos \theta'_W & \sin \theta'_W \\ \sin \theta_W \sin \theta'_W & -\cos \theta'_W \sin \theta'_W & \cos \theta'_W \end{pmatrix} \begin{pmatrix} A^Y \\ V^3 \\ A^X \end{pmatrix}. \quad (9)$$

We deduce  $\sin^2 \theta'_W$  as

$$\sin^2 \theta'_W = \frac{1}{2} - \frac{(g_{YX}^2 - g_1^2 - g_2^2)v^2 + 4g_X^2\xi^2}{2\sqrt{(g_{YX}^2 + g_1^2 + g_2^2)^2v^4 + 8g_X^2(g_{YX}^2 - g_1^2 - g_2^2)v^2\xi^2 + 16g_X^4\xi^4}}. \quad (10)$$

The new mixing angle  $\theta'_W$  appears in the couplings involving  $Z$  and  $Z'$ . The exact eigenvalues of Eq.(8) are calculated[19]

$$\begin{aligned} m_\gamma^2 &= 0, \\ m_{Z,Z'}^2 &= \frac{1}{8} \left( (g_1^2 + g_2^2 + g_{YX}^2)v^2 + 4g_X^2\xi^2 \right. \\ &\quad \left. \mp \sqrt{(g_1^2 + g_2^2 + g_{YX}^2)^2v^4 + 8(g_{YX}^2 - g_1^2 - g_2^2)g_X^2v^2\xi^2 + 16g_X^4\xi^4} \right). \end{aligned} \quad (11)$$

The Higgs potential is deduced here

$$\begin{aligned}
V = & \frac{1}{2}g_X(g_X + g_{YX})(|H_d^0|^2 - |H_u^0|^2)(|\eta|^2 - |\bar{\eta}|^2) + |\lambda_H|^2|H_u^0 H_d^0|^2 + m_S^2|S|^2 \\
& + \frac{1}{8}(g_1^2 + g_2^2 + (g_X + g_{YX})^2)(|H_d^0|^2 - |H_u^0|^2)^2 + \frac{1}{2}g_X^2(|\eta|^2 - |\bar{\eta}|^2)^2 + \lambda_C^2|\eta\bar{\eta}|^2 \\
& + (|\mu|^2 + |\lambda_H|^2|S|^2 + 2\text{Re}[\mu^*\lambda_H S])(|H_d^0|^2 + |H_u^0|^2) + |\lambda_C|^2|S|^2(|\eta|^2 + |\bar{\eta}|^2) \\
& + 2\text{Re}[l_W^*(2M_S S + \lambda_C \eta \bar{\eta} - \lambda_H H_u^0 H_d^0 + \kappa S^2)] + 4|M_S|^2|S|^2 + 2\text{Re}[\lambda_C^* \kappa \eta^* \bar{\eta}^* S^2] \\
& + |\kappa|^2|S|^4 + 4\text{Re}[M_S^* S^*(\lambda_C \eta \bar{\eta} - \lambda_H H_u^0 H_d^0 + \kappa S^2)] - 2\text{Re}[\lambda_C^* \lambda_H \eta^* \bar{\eta}^* H_u^0 H_d^0] + |l_W|^2 \\
& - 2\text{Re}[B_\mu H_d^0 H_u^0] + 2\text{Re}[L_S S] + \frac{2}{3}\text{Re}[T_k S^3] + 2\text{Re}[T_{\lambda_C} \eta \bar{\eta} S] - 2\text{Re}[T_{\lambda_H} H_d^0 H_u^0 S] \\
& - 2\text{Re}[\lambda_H \kappa^* H_u^0 H_d^0 (S^2)^*] + m_\eta^2|\eta|^2 + m_{\bar{\eta}}^2|\bar{\eta}|^2 + m_{H_u^0}^2|H_u^0|^2 + m_{H_d^0}^2|H_d^0|^2 + 2\text{Re}[B_S S^2]. \quad (12)
\end{aligned}$$

To simplify the following discussion, we suppose that the parameters  $(\mu, \lambda_H, \lambda_C, l_W, M_S, B_\mu, L_S, T_k, T_{\lambda_C}, T_{\lambda_H}, \kappa, B_S)$  in Eq.(12) are real parameters. The VEVs of the Higgs satisfy the following equations

$$\begin{aligned}
& \frac{1}{8}(g_1^2 + g_2^2 + (g_X + g_{YX})^2)(v_d^2 - v_u^2)v_d + \frac{1}{4}g_X(g_X + g_{YX})v_d(v_\eta^2 - v_{\bar{\eta}}^2) \\
& + (\mu^2 + \frac{1}{2}\lambda_H^2 v_S^2 + \sqrt{2}\mu\lambda_H v_S)v_d - l_W\lambda_H v_u + \frac{1}{2}\lambda_H^2 v_u^2 v_d - \sqrt{2}M_S\lambda_H v_S v_u \\
& - \frac{1}{2}\lambda_H\lambda_C v_\eta v_{\bar{\eta}} v_u - \frac{1}{2}\lambda_H\kappa v_u v_S^2 + m_{H_d}^2 v_d - B_\mu v_u - \frac{T_{\lambda_H}}{\sqrt{2}}v_u v_S = 0, \quad (13)
\end{aligned}$$

$$\begin{aligned}
& \frac{1}{8}(g_1^2 + g_2^2 + (g_X + g_{YX})^2)(v_u^2 - v_d^2)v_u + \frac{1}{4}g_X(g_X + g_{YX})v_u(v_\eta^2 - v_{\bar{\eta}}^2) \\
& + (\mu^2 + \frac{1}{2}\lambda_H^2 v_S^2 + \sqrt{2}\mu\lambda_H v_S)v_u - l_W\lambda_H v_d + \frac{1}{2}\lambda_H^2 v_u v_d^2 - \sqrt{2}M_S\lambda_H v_S v_d \\
& - \frac{1}{2}\lambda_H\lambda_C v_\eta v_{\bar{\eta}} v_d - \frac{1}{2}\lambda_H\kappa v_d v_S^2 + m_{H_u}^2 v_u - B_\mu v_d - \frac{T_{\lambda_H}}{\sqrt{2}}v_d v_S = 0, \quad (14)
\end{aligned}$$

$$\begin{aligned}
& \frac{1}{2}g_X^2(v_\eta^2 - v_{\bar{\eta}}^2)v_\eta - \frac{1}{4}g_X(g_X + g_{YX})v_\eta(v_u^2 - v_d^2) + \frac{1}{2}\lambda_C^2 v_\eta(v_S^2 + v_{\bar{\eta}}^2) + l_W\lambda_C v_{\bar{\eta}} \\
& + \sqrt{2}M_S\lambda_C v_S v_{\bar{\eta}} - \frac{1}{2}\lambda_H\lambda_C v_{\bar{\eta}} v_u v_d + \frac{1}{2}\lambda_C\kappa v_{\bar{\eta}} v_S^2 + m_{\eta}^2 v_\eta + \frac{T_{\lambda_H}}{\sqrt{2}}v_{\bar{\eta}} v_S = 0, \quad (15)
\end{aligned}$$

$$\begin{aligned}
& \frac{1}{2}g_X^2(v_{\bar{\eta}}^2 - v_\eta^2)v_{\bar{\eta}} + \frac{1}{4}g_X(g_X + g_{YX})v_{\bar{\eta}}(v_u^2 - v_d^2) + \frac{1}{2}\lambda_C^2 v_{\bar{\eta}}(v_S^2 + v_\eta^2) + l_W\lambda_C v_\eta \\
& + \sqrt{2}M_S\lambda_C v_S v_\eta - \frac{1}{2}\lambda_H\lambda_C v_\eta v_u v_d + \frac{1}{2}\lambda_C\kappa v_\eta v_S^2 + m_{\bar{\eta}}^2 v_{\bar{\eta}} + \frac{T_{\lambda_H}}{\sqrt{2}}v_\eta v_S = 0, \quad (16)
\end{aligned}$$

$$\begin{aligned}
& (\lambda_H^2 v_S + \sqrt{2}\mu\lambda_H)\frac{1}{2}v^2 + \frac{1}{2}\lambda_C^2 v_S \xi^2 + 4M_S^2 v_S + \kappa^2 v_S^3 + 2B_S v_S + \sqrt{2}L_S \\
& + 2l_W(\sqrt{2}M_S + \kappa v_S) + \sqrt{2}M_S(\lambda_C v_\eta v_{\bar{\eta}} - \lambda_H v_u v_d + 3\kappa v_S^2) + m_S^2 v_S \\
& + \lambda_C\kappa v_\eta v_{\bar{\eta}} v_S - \lambda_H\kappa v_u v_d v_S + \frac{1}{\sqrt{2}}(T_k v_S^2 + T_{\lambda_C} v_\eta v_{\bar{\eta}} - T_{\lambda_H} v_u v_d) = 0. \quad (17)
\end{aligned}$$

The neutrino mass matrix is deduced in the base  $(\nu_L, \bar{\nu}_R)$

$$M_\nu = \begin{pmatrix} 0 & \frac{v_u}{\sqrt{2}}(Y_\nu^T)^{IJ} \\ \frac{v_u}{\sqrt{2}}(Y_\nu)^{IJ} & \sqrt{2}v_{\bar{\eta}}(Y_X)^{IJ} \end{pmatrix}, \quad (18)$$

and it is diagonalized by the matrix  $Z_\nu$  through the formula

$$Z_\nu M_\nu Z_\nu^T = \text{diag}(M_\nu). \quad (19)$$

The mass matrix for CP-even sneutrino  $(\phi_l, \phi_r)$  reads as

$$M_{\bar{\nu}^R}^2 = \begin{pmatrix} m_{\phi_l \phi_l} & m_{\phi_r \phi_l}^T \\ m_{\phi_l \phi_r} & m_{\phi_r \phi_r} \end{pmatrix}, \quad (20)$$

$$m_{\phi_l \phi_l} = \frac{1}{8} \left( (g_1^2 + g_{YX}^2 + g_2^2 + g_{YX}g_X)(v_d^2 - v_u^2) + g_{YX}g_X(2v_\eta^2 - 2v_{\bar{\eta}}^2) \right) + \frac{1}{2}v_u^2 Y_\nu^T Y_\nu + m_L^2, \quad (21)$$

$$m_{\phi_l \phi_r} = \frac{1}{\sqrt{2}}v_u T_\nu + v_u v_{\bar{\eta}} Y_X Y_\nu - \frac{1}{2}v_d(\lambda_H v_S + \sqrt{2}\mu)Y_\nu, \quad (22)$$

$$m_{\phi_r \phi_r} = \frac{1}{8} \left( (g_{YX}g_X + g_X^2)(v_d^2 - v_u^2) + 2g_X^2(v_\eta^2 - v_{\bar{\eta}}^2) \right) + v_\eta v_S Y_X \lambda_C + m_{\bar{\nu}}^2 + \frac{1}{2}v_u^2 |Y_\nu|^2 + v_{\bar{\eta}}(2v_{\bar{\eta}} Y_X Y_X + \sqrt{2}T_X). \quad (23)$$

To obtain the masses of sneutrinos, we use  $Z^R$  to diagonalize  $M_{\bar{\nu}^R}^2$ .

The mass matrix for CP-odd sneutrino  $(\sigma_l, \sigma_r)$  is also deduced here

$$M_{\bar{\nu}^I}^2 = \begin{pmatrix} m_{\sigma_l \sigma_l} & m_{\sigma_r \sigma_l}^T \\ m_{\sigma_l \sigma_r} & m_{\sigma_r \sigma_r} \end{pmatrix}, \quad (24)$$

$$m_{\sigma_l \sigma_l} = \frac{1}{8} \left( (g_1^2 + g_{YX}^2 + g_2^2 + g_{YX}g_X)(v_d^2 - v_u^2) + 2g_{YX}g_X(v_\eta^2 - v_{\bar{\eta}}^2) \right) + \frac{1}{2}v_u^2 Y_\nu^T Y_\nu + m_L^2, \quad (25)$$

$$m_{\sigma_l \sigma_r} = \frac{1}{\sqrt{2}}v_u T_\nu - v_u v_{\bar{\eta}} Y_X Y_\nu - \frac{1}{2}v_d(\lambda_H v_S + \sqrt{2}\mu)Y_\nu, \quad (26)$$

$$m_{\sigma_r \sigma_r} = \frac{1}{8} \left( (g_{YX}g_X + g_X^2)(v_d^2 - v_u^2) + 2g_X^2(v_\eta^2 - v_{\bar{\eta}}^2) \right) - v_\eta v_S Y_X \lambda_C + m_{\bar{\nu}}^2 + \frac{1}{2}v_u^2 |Y_\nu|^2 + v_{\bar{\eta}}(2v_{\bar{\eta}} Y_X Y_X - \sqrt{2}T_X). \quad (27)$$

With the matrix  $Z^I$ , we can diagonalize the mass squared matrix of sneutrino  $M_{\bar{\nu}^I}^2$ .

The neutral CP-even Higgs  $\phi_d, \phi_u, \phi_\eta, \phi_{\bar{\eta}}$  and  $\phi_s$  mix together and form  $5 \times 5$  mass squared matrix. In the basis  $(\phi_d, \phi_u, \phi_\eta, \phi_{\bar{\eta}}, \phi_s)$ , the mass matrix reads as

$$m_h^2 = \begin{pmatrix} m_{\phi_d \phi_d} & m_{\phi_u \phi_d} & m_{\phi_\eta \phi_d} & m_{\phi_{\bar{\eta}} \phi_d} & m_{\phi_s \phi_d} \\ m_{\phi_d \phi_u} & m_{\phi_u \phi_u} & m_{\phi_\eta \phi_u} & m_{\phi_{\bar{\eta}} \phi_u} & m_{\phi_s \phi_u} \\ m_{\phi_d \phi_\eta} & m_{\phi_u \phi_\eta} & m_{\phi_\eta \phi_\eta} & m_{\phi_{\bar{\eta}} \phi_\eta} & m_{\phi_s \phi_\eta} \\ m_{\phi_d \phi_{\bar{\eta}}} & m_{\phi_u \phi_{\bar{\eta}}} & m_{\phi_\eta \phi_{\bar{\eta}}} & m_{\phi_{\bar{\eta}} \phi_{\bar{\eta}}} & m_{\phi_s \phi_{\bar{\eta}}} \\ m_{\phi_d \phi_s} & m_{\phi_u \phi_s} & m_{\phi_\eta \phi_s} & m_{\phi_{\bar{\eta}} \phi_s} & m_{\phi_s \phi_s} \end{pmatrix}. \quad (28)$$

To save space in the text, the concrete forms of the elements  $m_{\phi_d \phi_d}$  etc in this mass matrix are shown in the appendix. This matrix is diagonalized by  $Z^H$ .

The mass squared matrix for CP-odd Higgs in the basis  $(\sigma_d, \sigma_u, \sigma_\eta, \sigma_{\bar{\eta}}, \sigma_s)$  is shown here and diagonalized by  $Z^A$

$$m_{A^0}^2 = \begin{pmatrix} m_{\sigma_d \sigma_d} & m_{\sigma_u \sigma_d} & m_{\sigma_\eta \sigma_d} & m_{\sigma_{\bar{\eta}} \sigma_d} & m_{\sigma_s \sigma_d} \\ m_{\sigma_d \sigma_u} & m_{\sigma_u \sigma_u} & m_{\sigma_\eta \sigma_u} & m_{\sigma_{\bar{\eta}} \sigma_u} & m_{\sigma_s \sigma_u} \\ m_{\sigma_d \sigma_\eta} & m_{\sigma_u \sigma_\eta} & m_{\sigma_\eta \sigma_\eta} & m_{\sigma_{\bar{\eta}} \sigma_\eta} & m_{\sigma_s \sigma_\eta} \\ m_{\sigma_d \sigma_{\bar{\eta}}} & m_{\sigma_u \sigma_{\bar{\eta}}} & m_{\sigma_\eta \sigma_{\bar{\eta}}} & m_{\sigma_{\bar{\eta}} \sigma_{\bar{\eta}}} & m_{\sigma_s \sigma_{\bar{\eta}}} \\ m_{\sigma_d \sigma_s} & m_{\sigma_u \sigma_s} & m_{\sigma_\eta \sigma_s} & m_{\sigma_{\bar{\eta}} \sigma_s} & m_{\sigma_s \sigma_s} \end{pmatrix}. \quad (29)$$

The elements are also collected in the appendix.

In the same way, the mass matrix for slepton with the basis  $(\tilde{e}_L, \tilde{e}_R)$  is diagonalized by  $Z^E$  through the formula  $Z^E m_{\tilde{e}}^2 Z^{E,\dagger} = m_{2,\tilde{e}}^{diag}$ ,

$$m_{\tilde{e}}^2 = \begin{pmatrix} m_{\tilde{e}_L \tilde{e}_L^*} & \frac{1}{2}(\sqrt{2}v_d T_e^\dagger - v_u(\lambda_H x S + \sqrt{2}\mu)Y_e^\dagger) \\ \frac{1}{2}(\sqrt{2}v_d T_e - v_u Y_e(\sqrt{2}\mu^* + x S \lambda_H^*)) & m_{\tilde{e}_R \tilde{e}_R^*} \end{pmatrix}. \quad (30)$$

$$\begin{aligned} m_{\tilde{e}_L \tilde{e}_L^*} &= m_{\tilde{l}}^2 + \frac{1}{8}((g_1^2 + g_{YX}^2 + g_{YX}g_X - g_2^2)(v_d^2 - v_u^2) + 2g_{YX}g_X(v_\eta^2 - v_{\bar{\eta}}^2)) + \frac{1}{2}v_d^2 Y_e^\dagger Y_e, \\ m_{\tilde{e}_R \tilde{e}_R^*} &= m_e^2 - \frac{1}{8}([2(g_1^2 + g_{YX}^2) + 3g_{YX}g_X + g_X^2](v_d^2 - v_u^2) \\ &\quad + (4g_{YX}g_X + 2g_X^2)(v_\eta^2 - v_{\bar{\eta}}^2)) + \frac{1}{2}v_d^2 Y_e Y_e^\dagger. \end{aligned} \quad (31)$$

The mass matrix for neutralinos in the basis:  $(\lambda_{\tilde{B}}, \tilde{W}^0, \tilde{H}_d^0, \tilde{H}_u^0, \lambda_{\tilde{X}}, \tilde{\eta}, \tilde{\bar{\eta}}, \tilde{s})$  is,



$$m_{\tilde{\chi}^0} = \begin{pmatrix} M_1 & 0 & -\frac{g_1}{2}v_d & \frac{g_1}{2}v_u & M_{BB'} & 0 & 0 & 0 \\ 0 & M_2 & \frac{1}{2}g_2v_d & -\frac{1}{2}g_2v_u & 0 & 0 & 0 & 0 \\ -\frac{g_1}{2}v_d & \frac{1}{2}g_2v_d & 0 & m_{\tilde{H}_u^0\tilde{H}_d^0} & m_{\lambda_{\tilde{X}}\tilde{H}_d^0} & 0 & 0 & -\frac{\lambda_H v_u}{\sqrt{2}} \\ \frac{g_1}{2}v_u & -\frac{1}{2}g_2v_u & m_{\tilde{H}_d^0\tilde{H}_u^0} & 0 & m_{\lambda_{\tilde{X}}\tilde{H}_u^0} & 0 & 0 & -\frac{\lambda_H v_d}{\sqrt{2}} \\ M_{BB'} & 0 & m_{\tilde{H}_d^0\lambda_{\tilde{X}}} & m_{\tilde{H}_u^0\lambda_{\tilde{X}}} & M_{BL} & -g_X v_\eta & g_X v_{\bar{\eta}} & 0 \\ 0 & 0 & 0 & 0 & -g_X v_\eta & 0 & \frac{1}{\sqrt{2}}\lambda_C v_S & \frac{1}{\sqrt{2}}\lambda_C v_{\bar{\eta}} \\ 0 & 0 & 0 & 0 & g_X v_{\bar{\eta}} & \frac{1}{\sqrt{2}}\lambda_C v_S & 0 & \frac{1}{\sqrt{2}}\lambda_C v_\eta \\ 0 & 0 & -\frac{\lambda_H v_u}{\sqrt{2}} & -\frac{\lambda_H v_d}{\sqrt{2}} & 0 & \frac{1}{\sqrt{2}}\lambda_C v_{\bar{\eta}} & \frac{1}{\sqrt{2}}\lambda_C v_\eta & m_{\tilde{s}\tilde{s}} \end{pmatrix}, \quad (32)$$

$$m_{\tilde{H}_d^0\tilde{H}_u^0} = -\frac{1}{\sqrt{2}}\lambda_H v_S - \mu, \quad m_{\tilde{H}_d^0\lambda_{\tilde{X}}} = -\frac{1}{2}(g_{YX} + g_X)v_d, \quad (33)$$

$$m_{\tilde{H}_u^0\lambda_{\tilde{X}}} = \frac{1}{2}(g_{YX} + g_X)v_u, \quad m_{\tilde{s}\tilde{s}} = 2M_S + \sqrt{2}\kappa v_S. \quad (34)$$

This matrix is diagonalized by  $Z^N$ :

$$Z^{N*} m_{\tilde{\chi}^0} Z^{N\dagger} = m_{\tilde{\chi}^0}^{diag}. \quad (35)$$

Here, we show some needed couplings in this model. The CP-even Higgs couples with CP-even sneutrinos

$$\begin{aligned} \mathcal{L}_{H\tilde{\nu}^R\tilde{\nu}^R} &= H_i \tilde{\nu}_j^R \frac{i}{4} \left\{ \sum_{a,b=1}^3 \left[ -2\sqrt{2}Z_{kb}^{R*} Z_{j3+a}^{R*} (T_\nu)_{ab} Z_{i2}^H - 2\lambda_C v_S Z_{k3+b}^{R*} Z_{j3+a}^{R*} (Y_X)_{ab} Z_{i3}^H \right. \right. \\ &\quad \left. \left. - 2\sqrt{2}Z_{k3+b}^{R*} Z_{j3+a}^{R*} (T_X)_{ab} Z_{i4}^H - 2\lambda_C v_\eta Z_{k3+b}^{R*} Z_{j3+a}^{R*} (Y_X)_{ab} Z_{i5}^H \right] + [j \leftrightarrow k] \right. \\ &\quad \left. - 16v_{\bar{\eta}} \sum_{a,b,c=1}^3 Z_{k3+c}^{R*} Z_{j3+b}^{R*} (Y_X)_{ac} (Y_X)_{ab} Z_{i4}^H + \sum_{a=1}^3 Z_{ka}^{R*} Z_{ja}^{R*} [(g_{YX}g_X + g_1^2 \right. \right. \\ &\quad \left. \left. + g_{YX}^2 + g_2^2)(-v_d Z_{i1}^H + v_u Z_{i2}^H) - 2g_{YX}g_X(-v_{\bar{\eta}} Z_{i4}^H + v_\eta Z_{i3}^H)] \right. \right. \\ &\quad \left. \left. + \sum_{a=1}^3 Z_{k3+a}^{R*} Z_{j3+a}^{R*} [(g_{YX}g_X + g_X^2)(v_u Z_{i2}^H - v_d Z_{i1}^H) - 2g_X^2(v_\eta Z_{i3}^H - v_{\bar{\eta}} Z_{i4}^H)] \right] \right\} \tilde{\nu}_k^{*R}. \quad (36) \end{aligned}$$

The CP-odd Higgs interact with  $\tilde{\nu}^I$  and  $\tilde{\nu}^R$ , whose concrete form is

$$\begin{aligned} \mathcal{L}_{A\tilde{\nu}^I\tilde{\nu}^R} &= A_i \tilde{\nu}_j^I \frac{i}{4} \sum_{a,b=1}^3 \left\{ \left[ 2v_S \lambda_C Z_{k3+b}^{R*} Z_{j3+a}^{I*} (Y_X)_{ab} Z_{i3}^A - 2\sqrt{2}Z_{kb}^{R*} Z_{j3+a}^{I*} (T_\nu)_{ab} Z_{i2}^A \right. \right. \\ &\quad \left. \left. - 2\sqrt{2}Z_{k3+b}^{R*} Z_{j3+a}^{I*} (T_X)_{ab} Z_{i4}^A + 2v_\eta \lambda_C Z_{k3+b}^{R*} Z_{j3+a}^{I*} (Y_X)_{ab} Z_{i5}^A \right] + [R \leftrightarrow I, j \leftrightarrow k] \right\} \tilde{\nu}_k^{*R}. \quad (37) \end{aligned}$$

The coupling of two CP-even Higgs and two CP-even sneutrinos reads as

$$\begin{aligned}
\mathcal{L}_{HH\tilde{\nu}^R\tilde{\nu}^R} &= H_i\tilde{\nu}_l^R \left\{ \frac{i}{2} \sum_{a,b=1}^3 \left[ \left( -\lambda_C Z_{l3+b}^{R*} Z_{k3+a}^{R*} (Y_X)_{ab} (Z_{i5}^H Z_{j3}^H + Z_{i3}^H Z_{j5}^H) \right) + (l \leftrightarrow k) \right] \right. \\
&+ \frac{i}{4} \sum_{a=1}^3 Z_{l3+a}^{R*} Z_{k3+a}^{R*} \left[ (g_{YX} g_X + g_X^2) (Z_{i2}^H Z_{j2}^H - Z_{i1}^H Z_{j1}^H) - 2g_X^2 (Z_{i3}^H Z_{j3}^H - Z_{i4}^H Z_{j4}^H) \right] \\
&+ \frac{i}{4} \sum_{a=1}^3 Z_{la}^{R*} Z_{ka}^{R*} \left[ (g_{YX} g_X + g_1^2 + g_{YX}^2 + g_2^2) (-Z_{i1}^H Z_{j1}^H + Z_{i2}^H Z_{j2}^H) \right. \\
&\left. \left. - 2g_{YX} g_X (Z_{i3}^H Z_{j3}^H - Z_{i4}^H Z_{j4}^H) \right] - 4i \sum_{a,b,c=1}^3 Z_{l3+c}^{R*} Z_{k3+b}^{R*} (Y_X)_{ab} (Y_X)_{ac} Z_{i4}^H Z_{j4}^H \right\} H_k \tilde{\nu}_k^R. \quad (38)
\end{aligned}$$

We also deduce the vertexes of  $\tilde{\nu}_k^R - \bar{e}_i - \chi_j^-$  and  $\tilde{\nu}_k^R - \nu_i - \bar{\chi}_i^0$ ,

$$\mathcal{L}_{\tilde{\nu}^R \bar{e} \chi^-} = \bar{e}_i \left\{ \frac{i}{\sqrt{2}} U_{j2}^* Z_{ki}^{R*} Y_e^i P_L - \frac{i}{\sqrt{2}} g_2 V_{j1} Z_{ki}^{R*} P_R \right\} \chi_j^- \tilde{\nu}_k^R, \quad (39)$$

$$\begin{aligned}
\mathcal{L}_{\tilde{\nu}^R \nu \bar{\chi}^0} &= \bar{\chi}_i^0 \left\{ \frac{i}{2} (-g_2 Z_{i2}^{N*} + g_{YX} Z_{i5}^{N*} + g_1 Z_{i1}^{N*}) \sum_{a=1}^3 Z_{ka}^{R*} U_{ja}^{V*} P_L \right. \\
&\left. + \frac{i}{2} (-g_2 Z_{i2}^N + g_{YX} Z_{i5}^N + g_1 Z_{i1}^N) \sum_{a=1}^3 Z_{ka}^{R*} U_{ja}^V P_R \right\} \nu_i \tilde{\nu}_k^R. \quad (40)
\end{aligned}$$

To save space in the text, we collect the other vertexes in the appendix.

### III. RELIC DENSITY

In this subsection, we suppose the lightest mass eigenstate ( $\tilde{\nu}_1^R$ ) of CP-even sneutrino mass squared matrix in Eq.(20) as a dark matter candidate and calculate the relic density. Any WIMP candidate has to satisfy the relic density constraints. The  $\tilde{\nu}_1^R$  number density  $n_{\tilde{\nu}_1^R}$  is governed by the Boltzmann equation[20, 21]

$$\frac{dn_{\tilde{\nu}_1^R}}{dt} = -3Hn_{\tilde{\nu}_1^R} - \langle \sigma v \rangle_{SA} (n_{\tilde{\nu}_1^R}^2 - n_{\tilde{\nu}_1^R eq}^2) - \langle \sigma v \rangle_{CA} (n_{\tilde{\nu}_1^R} n_\phi - n_{\tilde{\nu}_1^R eq} n_{\phi eq}). \quad (41)$$

$\tilde{\nu}_1^R$  can both self-annihilate and co-annihilate with another species  $\phi$ . When the annihilation rate of  $\tilde{\nu}_1^R$  becomes roughly equal to the Hubble expansion rate, the species freeze out at the temperature  $T_f$ .

$$\langle \sigma v \rangle_{SA} n_{\tilde{\nu}_1^R} + \langle \sigma v \rangle_{CA} n_\phi \sim H(T_f). \quad (42)$$

With the supposition  $M_\phi > M_{\tilde{\nu}_1^R}$  [22]

$$n_\phi = \left( \frac{M_\phi}{M_{\tilde{\nu}_1^R}} \right)^{3/2} \text{Exp}[(M_{\tilde{\nu}_1^R} - M_\phi)/T] n_{\tilde{\nu}_1^R}. \quad (43)$$

Then it becomes

$$\left[ \langle \sigma v \rangle_{SA} + \langle \sigma v \rangle_{CA} \left( \frac{M_\phi}{M_{\tilde{\nu}_1^R}} \right)^{3/2} \text{Exp}[(M_{\tilde{\nu}_1^R} - M_\phi)/T] \right] n_{\tilde{\nu}_1^R} \sim H(T_f). \quad (44)$$

We study its annihilation rate  $\langle \sigma v \rangle_{SA}$  and  $\langle \sigma v \rangle_{CA}$  and its relic density  $\Omega_D$  by the thermal dynamics of the Universe. The self-annihilation cross section  $\sigma(\tilde{\nu}_1^R \tilde{\nu}_1^{R*} \rightarrow \text{anything})$  and co-annihilation cross section  $\sigma(\tilde{\nu}_1^R \phi \rightarrow \text{anything})$  should be calculated. In the center of mass frame, their results can be written as  $\sigma v_{rel} = a + b v_{rel}^2$ , with  $v_{rel}$  denoting the relative velocity of the two particles in the initial states. It is a good approximation, to calculate the freeze-out temperature( $T_F$ ) from[23, 24] the following formula

$$x_F = \frac{m_D}{T_F} \simeq \ln \left[ \frac{0.038 M_{Pl} m_D (a + 6b/x_F)}{\sqrt{g_*} x_F} \right]. \quad (45)$$

$M_{Pl}$  is the Planck mass  $1.22 \times 10^{19}$  GeV.  $m_D = m_{\tilde{\nu}_1^R}$  denotes the WIMP mass and  $x_F \equiv m_D/T_F$ .  $g_*$  is the number of the relativistic degrees of freedom with mass less than  $T_F$ . The formula for the density of cold non-baryonic matter can be simplified in the following form[25]

$$\Omega_D h^2 \simeq \frac{1.07 \times 10^9 x_F}{\sqrt{g_*} M_{PL} (a + 3b/x_F) \text{GeV}}, \quad (46)$$

and its value should be  $\Omega_D h^2 = 0.1186 \pm 0.0020$  [7].

The dominate processes for the self-annihilation are:  $\tilde{\nu}_1^R + \tilde{\nu}_1^R \rightarrow \{(W+W), (Z+Z), (h^0 + h^0), (\bar{u}_i + u_i), (\bar{d}_i + d_i), (\bar{l}_i + l_i), (\bar{\nu}_i + \nu_i)\}$  with  $i = 1, 2, 3$ ,  $h^0$  representing the lightest CP-even Higgs.  $\nu_i$  denote three light neutrinos. The studied co-annihilation processes read as:  $\tilde{\nu}_1^R + \tilde{\nu}_1^I \rightarrow \{(W+W), (Z+h^0), (\bar{u}_i + u_i), (\bar{d}_i + d_i), (\bar{l}_i + l_i), (\bar{\nu}_i + \nu_i)\}$ , where  $\tilde{\nu}_1^I$  is the lightest mass eigenstate of CP-odd sneutrino mass squared matrix.

#### IV. DIRECT DETECTION

The main scattering processes of CP-even sneutrinos off nucleons are  $\tilde{\nu}^R + q \rightarrow \tilde{\nu}^R + q$  and  $\tilde{\nu}^R + q \rightarrow \tilde{\nu}^I + q$ . They can be divided into two types: exchange of CP-even Higgs bosons and gauge bosons( $Z, Z'$ ). For the first type process  $\tilde{\nu}^R + q \rightarrow \tilde{\nu}^R + q$ , the exchanged particles are CP-even Higgs. While for the second type process  $\tilde{\nu}^R + q \rightarrow \tilde{\nu}^I + q$ , the exchanged particles are vector bosons  $Z$  and  $Z'$ . The CP-odd Higgs boson contributions are much

smaller than the contributions from CP-even Higgs boson and can be neglected safely[26]. After the deduction, we obtain the operators  $\tilde{\nu}^{R*}\tilde{\nu}^R\bar{q}q$  and  $\tilde{\nu}^{R*}\partial_\mu\tilde{\nu}^R\bar{q}\gamma^\mu q$  at the quark level.

To get the final results, we should convert the quark level coupling to the effective nucleon coupling. For the operator  $\tilde{\nu}^{R*}\tilde{\nu}^R\bar{q}q$ , the used formulae are shown here[26]

$$\begin{aligned} a_q m_q \bar{q}q &\rightarrow f_N m_N \bar{N}N, & f_N &= \sum_{q=u,d,s} f_{Tq}^{(N)} a_q + \frac{2}{27} f_{TG}^{(N)} \sum_{q=c,b,t} a_q, \\ \langle N | m_q \bar{q}q | N \rangle &= m_N f_{Tq}^{(N)}, & f_{TG}^{(N)} &= 1 - \sum_{q=u,d,s} f_{Tq}^{(N)}. \end{aligned} \quad (47)$$

Here,  $f_N$  includes the coupling to gluons induced by integrating out heavy quark loops. The numbers of  $f_{Tq}^{(N)}$  are collected here, which are used by the DarkSUSY package[27],

$$\begin{aligned} f_{Tu}^{(p)} &= 0.023, & f_{Td}^{(p)} &= 0.034, & f_{Ts}^{(p)} &= 0.14, \\ f_{Tu}^{(n)} &= 0.019, & f_{Td}^{(n)} &= 0.041, & f_{Ts}^{(n)} &= 0.14. \end{aligned} \quad (48)$$

It is easy to convert the operator  $b_q \tilde{\nu}^{R*}\partial_\mu\tilde{\nu}^R\bar{q}\gamma^\mu q$  to  $b_N \tilde{\nu}^{R*}\partial_\mu\tilde{\nu}^R\bar{N}\gamma^\mu N$  through the following formulas

$$b_p = 2b_u + b_d, \quad b_n = 2b_d + b_u. \quad (49)$$

With the obtained  $f_N$ , one gets the nucleon cross section

$$\sigma = \frac{1}{\pi} \mu^2 [Z_p f_p + (A - Z_p) f_n]^2. \quad (50)$$

Here  $Z_p$  is the number of proton, and  $A$  represents the number of atom.

## V. NUMERICAL RESULTS

In this section, we study the numerical results. The used parameters are supposed as the following

$$\begin{aligned} \mu &= M_S = T_\kappa = M_1 = M_2 = 1 \text{ TeV}, & \tan\beta &= 5, & v_\eta &= 2 \text{ TeV}, & v_{\bar{\eta}} &= 0.9 \text{ TeV}, \\ \lambda_C &= -0.5, & v_S &= 3 \text{ TeV}, & T_{\lambda_H} &= 2 \text{ TeV}, & l_W = B_\mu = B_S = m_S^2 &= 1 \text{ TeV}^2, \\ T_{\nu 22} &= 2 \text{ TeV}, & T_{\nu 33} &= 3 \text{ TeV}, & M_{\nu 11} &= 1176^2 \text{ GeV}^2, & T_{\lambda_C} &= 1.2 \text{ TeV}, \\ M_{\nu 22} &= 2 \text{ TeV}^2, & M_{\nu 33} &= 3 \text{ TeV}^2, & T_{X 22} = T_{X 33} &= 1.1 \text{ TeV}, & \kappa &= 0.7, \\ M_L = M_E &= \delta_{ij} 10 \text{ TeV}^2 \text{ and } T_e = \delta_{ij} \text{ TeV and } Y_X = \delta_{ij} 0.5, & (i, j &= 1, 2, 3). \end{aligned} \quad (51)$$

Here, we take  $T_\nu$ ,  $T_X$  and  $M_\nu$  as diagonal matrices, for example

$$T_\nu = \begin{pmatrix} T_{\nu 11} & 0 & 0 \\ 0 & T_{\nu 22} & 0 \\ 0 & 0 & T_{\nu 33} \end{pmatrix}. \quad (52)$$

Firstly, we research the CP-even Higgs masses at tree level, especially for the lightest Higgs mass. Secondly, the relic density of the lightest CP-even sneutrino is calculated numerically. At last, we study the cross section for the lightest sneutrino scattering from nucleon.

### A. tree level Higgs mass

The mixing mass squared matrix for CP-even Higgs at tree level is shown in the Eq.(28). It is well known that, in MSSM the lightest CP-even Higgs at tree level can be no more than 90 GeV. To match the Higgs mass with 125.1 GeV detected at LHC, the loop corrections must be considered. However, in  $U(1)_X SSM$  there are three new Higgs superfields beyond MSSM, and  $U(1)_X SSM$  can improve the CP-even Higgs mass at tree level. Using the parameters,  $T_{\nu 11} = 1$  TeV,  $T_{X 11} = 1.1$  TeV,  $M_{BL} = 1$  TeV,  $M_{BB'} = 0.1$  TeV, we study the five CP-even Higgs mass eigenstates. The lightest CP-even Higgs mass is denoted by  $m_h$ .

In Fig.(1), with  $g_{YX} = 0.15$ ,  $m_h$  versus  $\lambda_H$  is plotted by the solid line( $g_X = 0.3$ ) and dotted line( $g_X = 0.2$ ) respectively. The two lines possess similar behaviors with the varying  $\lambda_H$ . The solid line is above the dotted line and the largest value of the solid line is about 106 GeV as  $\lambda_H = 0.6$ . With  $g_X = 0.2$ , the mass region for the other four Higgs masses are respectively  $m_{H^1}(6611 \sim 8283)$  GeV,  $m_{H^2}(5220 \sim 6609)$  GeV,  $m_{H^3} \sim 2036$  GeV and  $m_{H^4} \sim 640$  GeV. While,  $m_{H^1}(6611 \sim 8293)$  GeV,  $m_{H^2}(5220 \sim 6609)$  GeV,  $m_{H^3} \sim 2066$  GeV and  $m_{H^4} \sim 725$  GeV correspond to  $g_X = 0.3$ . In general,  $m_{H^1}, m_{H^2}$  and  $m_{H^3}$  are all very heavy with the used parameters.

$g_{YX}$  is the parameter for the mixing of  $U(1)_Y$  and  $U(1)_X$ , and it is very important for the tree level Higgs mass  $m_h$ . Because the VEVs  $v_\eta$  and  $v_{\bar{\eta}}$  are large, which indicates that both of them can make large contributions to  $m_h$  at the tree level through  $g_{YX}$ . With  $\lambda_H = 0.5$ , we plot the numerical results for  $m_h$  versus  $g_{YX}$  by the solid line ( $g_X = 0.3$ ) and dotted line ( $g_X = 0.2$ ), respectively. The solid line and dotted line are very near, and they are both increasing functions with the enlarging  $g_{YX}$ . Near the point  $g_{YX} = 0.5$ ,  $m_h$  can almost reach

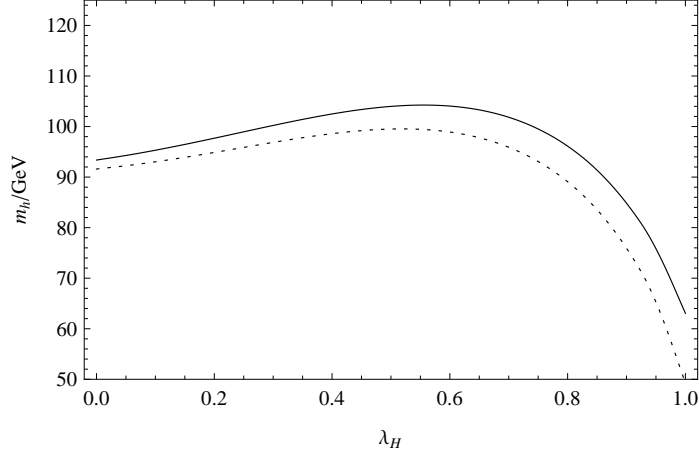


FIG. 1: The lightest CP-even Higgs mass versus  $\lambda_H$  with  $g_X = 0.3$  (solid line) and  $g_X = 0.2$  (dashed line) respectively.

125 GeV, without the loop corrections. In some SUSY models, the lightest CP-even Higgs must receive large loop corrections to match  $m_h = 125.1$  GeV. So, it is interesting that in this model the loop contributions to Higgs mass can be small. The other Higgs masses are very stable with the varying  $g_{YX}$  and  $m_{H^1} \sim 6930$  GeV,  $m_{H^2} \sim 6602$  GeV,  $m_{H^3} \sim 2036$  GeV,  $m_{H^4} \sim 640$  GeV for  $g_X = 0.2$ . The corresponding values for  $g_X = 0.3$  are respectively  $m_{H^1} \sim 6931$  GeV,  $m_{H^2} \sim 6602$  GeV,  $m_{H^3} \sim 2066$  GeV,  $m_{H^4} \sim 725$  GeV.

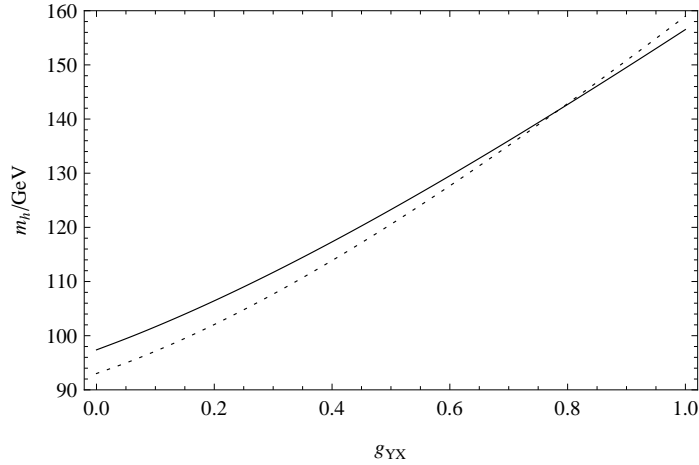


FIG. 2: The lightest CP-even Higgs mass versus  $g_{YX}$  with  $g_X = 0.3$  (solid line) and  $g_X = 0.2$  (dashed line) respectively.

## B. relic density of sneutrino dark matter

Here, the relic density of sneutrino dark matter are analyzed numerically, with the parameters  $g_X = 0.2$ ,  $g_{YX} = 0.15$  and  $\lambda_H = 0.5$ .  $T_\nu$  is the triplet coupling parameter appearing in the sneutrino mass squared matrix. In Fig.(3), we adopt  $T_{X11} = 1.1$  TeV,  $M_{BL} = 1$  TeV,  $M_{BB'} = 0.1$  TeV and study the relic density versus  $T_{\nu 11}$ . From the numerical calculation, we find that the virtual Higgs contributions to the relic density are about four orders smaller than the contributions from virtual  $Z$  and  $Z'$ . Therefore, we neglect the Higgs contributions. The gray area in the left diagram of the Fig.(3) represents the experimental value of the relic density in three  $\sigma$  and the solid line denotes the relic density which is the decreasing function of  $T_{\nu 11}$ . When  $T_{\nu 11}$  is around 1000 GeV, the relic density can reach the central value of the experiments. In the right diagram of Fig.(3), the numerical results of  $x_F$  versus  $T_{\nu 11}$  are plotted by the solid line, which is very stable and varies from 23.65 to 23.8.

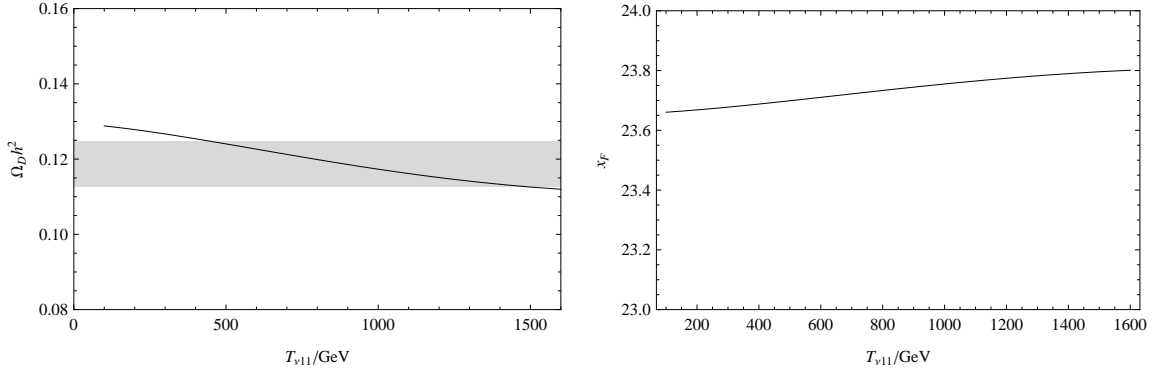


FIG. 3: The relic density and  $x_F$  versus  $T_{\nu 11}$ .

$M_{BL}$  is the mass of super partner for the new gauge boson.  $M_{BL}$  and  $M_{BB'}$  both influence the masses of neutralinos, so they affect the relic density of sneutrino dark matter through neutralino contribution. For  $T_{X11} = 1.1$  TeV and  $T_{\nu 11} = 1$  TeV, the relic density and  $x_F$  varying with  $M_{BL}$  are represented by the solid line ( $M_{BB'} = 100$  GeV) and dotted line ( $M_{BB'} = 500$  GeV) in the Fig.(4). From the right diagram of Fig.(4), it is obvious that the region of  $M_{BL}$  in 1000 GeV to 2000 GeV is more rational. The  $x_F$  region in the right diagram is from 23.6 to 23.8.

$T_X$  is the triplet coupling constant of  $\tilde{\nu}_R$  and  $\bar{\eta}$ , which can affect the sneutrino masses and couplings. Therefore, we research how  $T_{X11}$  the first element of  $T_X$  impact on the numerical results of the relic density. From the left diagram of Fig.(5), one can easily see that both

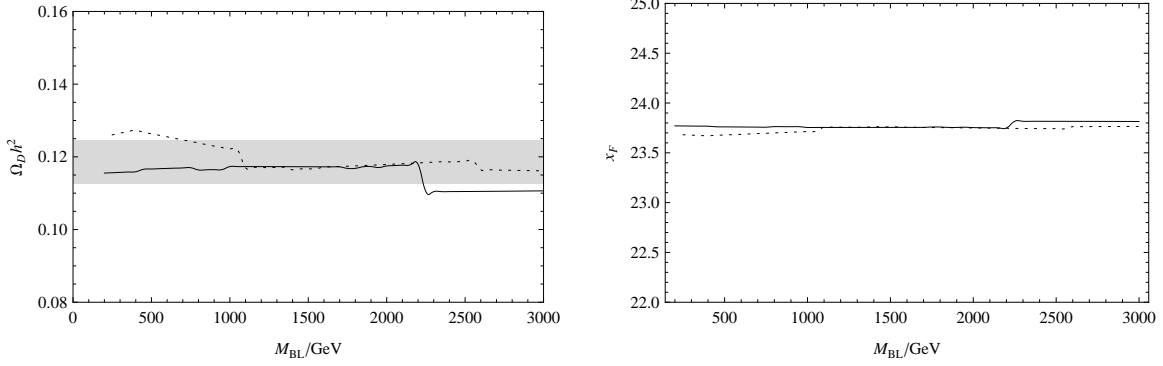


FIG. 4: The relic density and  $x_F$  versus  $M_{BL}$ , with  $M_{BB'}=100\text{GeV}$  (solid line) and  $M_{BB'}=500\text{GeV}$  (dashed line)

the solid line ( $M_{BB'} = 100\text{GeV}$ ) and dotted line ( $M_{BB'} = 500\text{GeV}$ ) are increasing functions of  $T_{X11}$ . In the left diagram, the dotted line is a little bigger than the solid line for the same value of  $T_{X11}$ . To matching the experimental value well,  $T_{X11}$  should be near 1000 GeV. On the contrary,  $x_F$  is the decreasing function of  $T_{X11}$  in the right diagram of Fig.(5), where the solid line and the dotted line are very near. Their region is from 23.65 to 23.87.

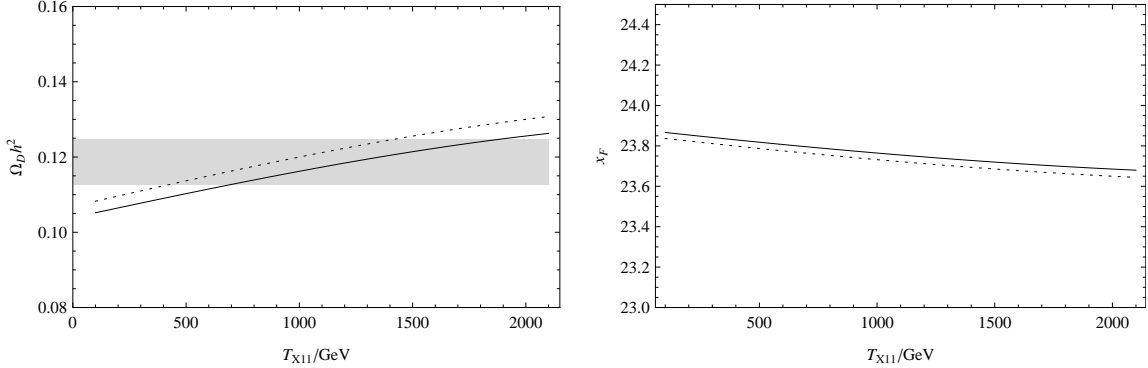


FIG. 5: The relic density and  $x_F$  versus  $T_{X11}$ , with  $M_{BB'}=100\text{GeV}$  (solid line) and  $M_{BB'}=400\text{GeV}$  (dashed line)

### C. the cross section of the sneutrino scattering off nucleon

In this subsection, taking into account the constraint from the relic density, we numerically calculate the cross section of sneutrino scattering from nucleon. We take the parameters



as  $T_{\nu 11} = 1$  TeV,  $T_{X11} = 1.1$  TeV,  $M_{BL} = 1$  TeV,  $M_{BB'} = 0.1$  TeV and  $\lambda_H = 0.5$ . As discussed in the front parts,  $g_X$  and  $g_{YX}$  are both important parameters, in the Fig.(6) the numerical results of the cross section versus  $g_X$  are plotted by the solid line( $g_{YX} = 0.15$ ) and dotted line( $g_{YX} = 0.25$ ) respectively. In these parameter space, the lightest CP-even sneutrino is at the order of 1000 GeV, whose experiment limit for the cross section is about  $10^{-46}\text{cm}^2$ . The dotted line is above the solid line, and they both turn large with the increasing  $g_X$ . According to the solid line, it is better for  $g_X$  to be no more than 0.3. When  $g_X < 0.1$ , the numerical results of the cross section are at the order of  $10^{-47}\text{cm}^2$  and even smaller.

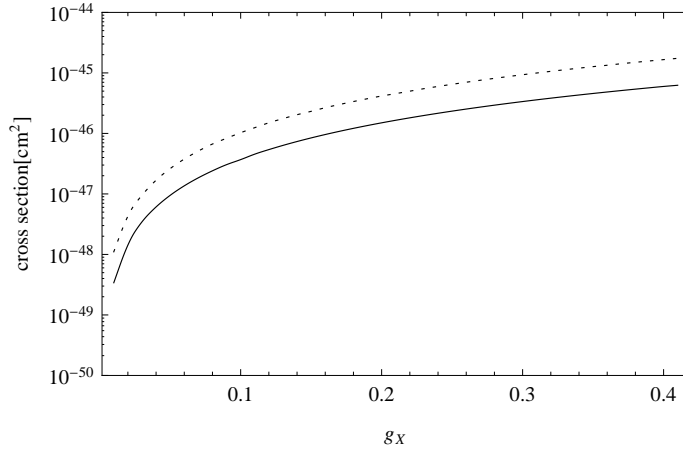


FIG. 6: The cross section versus  $g_X$  with  $g_{YX} = 0.15$ (solid line) and  $g_{YX} = 0.25$ (dotted line) respectively.

In the Fig.(7), the solid line ( $g_X = 0.15$ ) and dotted line ( $g_X = 0.2$ ) increase with the enlarging  $g_{YX}$ . The characters of the Fig.(7) are similar as those of Fig.(6). From the both Figs. (6) and (7), one can find that  $g_X$  and  $g_{YX}$  are important parameters to produce increasing effects. From the above discussion, when  $g_X$  and  $g_{YX}$  are no more than 0.3, the theoretical predictions can easily satisfy the experimental bounds.

## VI. DISCUSSION AND CONCLUSION

$U(1)_X$ SSM is the extension of MSSM, and the local gauge group of  $U(1)_X$ SSM is  $SU(3)_C \times SU(2)_L \times U(1)_Y \times U(1)_X$ . To obtain this model, right-handed neutrinos and three Higgs superfields  $\hat{\eta}$ ,  $\hat{\bar{\eta}}$ ,  $\hat{S}$  are added to the MSSM. Through the see-saw mechanism, three tiny

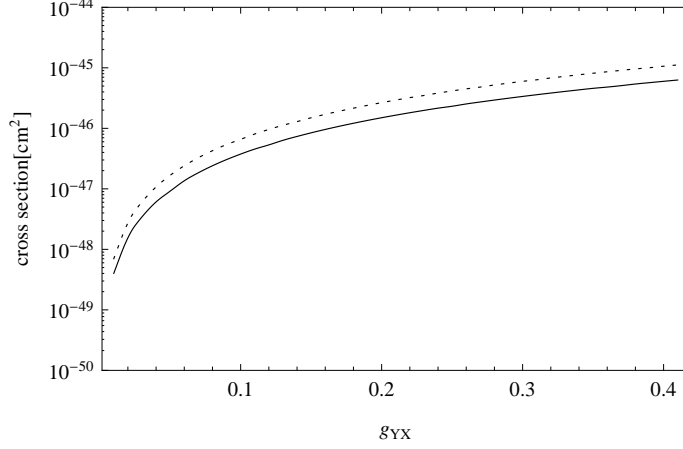


FIG. 7: The cross section versus  $g_{YX}$  with  $g_X = 0.15$ (solid line) and  $g_X = 0.2$ (dotted line) respectively.

neutrino masses can be produced. The right-handed sneutrinos are sterile, and if they are main parts of the lightest sneutrino, it possesses the characters of cold dark matter.

In  $U(1)_X$ SSM, we study the CP-even Higgs masses at tree level. Due to the introduction of Higgs superfields  $\hat{\eta}$ ,  $\hat{\bar{\eta}}$ ,  $\hat{S}$ , at tree level the lightest CP-even Higgs mass can be larger than that in MSSM. With the assumption that the lightest CP-even sneutrino can be cold dark matter candidate, the relic density of dark matter and the cross section of dark matter scattering from nucleon are both studied. The virtual Higgs contributions to both the relic density and the scattering cross section from nucleon are several orders smaller than those from virtual  $Z$  and  $Z'$ , so these type contributions can be neglected. The numerical results imply that the gauge coupling parameters  $g_X$  and  $g_{YX}$  are important. The used parameter space can satisfy the dark matter experimental constraints from both the relic density and the scattering from nucleon. This work gives constraints to the parameter space of  $U(1)_X$ SSM and may be benefit for the detection of dark matter.

### Acknowledgments

We are very grateful to Wei Chao the professor of Beijing Normal University, for giving us some useful discussions. This work is supported by National Natural Science Foundation of China (NNSFC) (No. 11535002, No. 11605037, No. 11705045), Post-graduate's Innovation Fund Project of Hebei Province (No. CXZZBS2019027), Hebei Key Lab of Optic-Electronic Information and Materials, and the youth top-notch talent support program of the Hebei Province.

## Appendix

The elements in the CP-even Higgs mass squared matrix

$$\begin{aligned}
m_{\phi_d \phi_d} &= m_{H_d}^2 + |\mu|^2 + \frac{1}{8} \left( [g_1^2 + (g_X + g_{YX})^2 + g_2^2] (3v_d^2 - v_u^2) \right. \\
&\quad \left. + 2(g_{YX}g_X + g_X^2)(v_\eta^2 - v_{\bar{\eta}}^2) \right) + \sqrt{2}v_S\mu\lambda_H + \frac{1}{2}(v_u^2 + v_S^2)|\lambda_H|^2, \\
m_{\phi_d \phi_u} &= -\frac{1}{4} \left( g_2^2 + (g_{YX} + g_X)^2 + g_1^2 \right) v_d v_u + |\lambda_H|^2 v_d v_u - \lambda_H l_W \\
&\quad - \frac{1}{2} \lambda_H (v_\eta v_{\bar{\eta}} \lambda_C + v_S^2 \kappa) - B_\mu - \sqrt{2}v_S \left( \frac{1}{2} T_{\lambda_H} + M_S \lambda_H \right), \\
m_{\phi_u \phi_u} &= m_{H_u}^2 + |\mu|^2 + \frac{1}{8} \left( [g_1^2 + (g_X + g_{YX})^2 + g_2^2] (3v_u^2 - v_d^2) \right. \\
&\quad \left. + 2(g_{YX}g_X + g_X^2)(v_\eta^2 - v_{\bar{\eta}}^2) \right) + \sqrt{2}v_S\mu\lambda_H + \frac{1}{2}(v_d^2 + v_S^2)|\lambda_H|^2, \\
m_{\phi_d \phi_\eta} &= \frac{1}{2} g_X (g_{YX} + g_X) v_d v_\eta - \frac{1}{2} v_u v_{\bar{\eta}} \lambda_H \lambda_C, \\
m_{\phi_u \phi_\eta} &= -\frac{1}{2} g_X (g_{YX} + g_X) v_u v_\eta - \frac{1}{2} v_d v_{\bar{\eta}} \lambda_H \lambda_C, \\
m_{\phi_\eta \phi_\eta} &= m_\eta^2 + \frac{1}{4} \left( (g_{YX}g_X + g_X^2)(v_d^2 - v_u^2) + 2g_X^2(3v_\eta^2 - v_{\bar{\eta}}^2) \right) + \frac{|\lambda_C|^2}{2}(v_\eta^2 + v_{\bar{\eta}}^2), \\
m_{\phi_d \phi_{\bar{\eta}}} &= -\frac{1}{2} g_X (g_{YX} + g_X) v_d v_{\bar{\eta}} - \frac{1}{2} v_u v_\eta \lambda_H \lambda_C, \\
m_{\phi_u \phi_{\bar{\eta}}} &= \frac{1}{2} g_X (g_{YX} + g_X) v_u v_{\bar{\eta}} - \frac{1}{2} v_d v_\eta \lambda_H \lambda_C, \\
m_{\phi_\eta \phi_{\bar{\eta}}} &= -g_X^2 v_\eta v_{\bar{\eta}} + \frac{1}{2} (2l_W - \lambda_H v_d v_u) \lambda_C + |\lambda_C|^2 v_\eta v_{\bar{\eta}} \\
&\quad + \frac{1}{\sqrt{2}} v_S (2M_S \lambda_C + T_{\lambda_C}) + \frac{1}{2} v_S^2 \lambda_C \kappa, \\
m_{\phi_{\bar{\eta}} \phi_{\bar{\eta}}} &= m_{\bar{\eta}}^2 + \frac{1}{4} \left( (g_{YX}g_X + g_X^2)(v_u^2 - v_d^2) + 2g_X^2(3v_{\bar{\eta}}^2 - v_\eta^2) \right) + \frac{|\lambda_C|^2}{2}(v_{\bar{\eta}}^2 + v_\eta^2), \\
m_{\phi_d \phi_s} &= \left( \lambda_H v_d v_S + \sqrt{2}v_d \mu - v_u (\kappa v_S + \sqrt{2}M_S) \right) \lambda_H - \frac{1}{\sqrt{2}} v_u T_{\lambda_H}, \\
m_{\phi_u \phi_s} &= \left( \lambda_H v_u v_S + \sqrt{2}v_u \mu - v_d (\kappa v_S + \sqrt{2}M_S) \right) \lambda_H - \frac{1}{\sqrt{2}} v_d T_{\lambda_H}, \\
m_{\phi_\eta \phi_s} &= \left( \lambda_C v_\eta v_S + v_{\bar{\eta}} (\kappa v_S + \sqrt{2}M_S) \right) \lambda_C + \frac{1}{\sqrt{2}} v_{\bar{\eta}} T_{\lambda_C}, \\
m_{\phi_{\bar{\eta}} \phi_s} &= \left( \lambda_C v_{\bar{\eta}} v_S + v_\eta (\kappa v_S + \sqrt{2}M_S) \right) \lambda_C + \frac{1}{\sqrt{2}} v_\eta T_{\lambda_C}, \\
m_{\phi_s \phi_s} &= m_S^2 + \left( 2l_W + 3v_S (\kappa v_S + 2\sqrt{2}M_S) + \lambda_C v_\eta v_{\bar{\eta}} - \lambda_H v_d v_u \right) \kappa \\
&\quad + \frac{1}{2} |\lambda_C|^2 \xi^2 + \frac{1}{2} |\lambda_H|^2 v^2 + 2B_S + 4|M_S|^2 + \sqrt{2}v_S T_\kappa.
\end{aligned} \tag{53}$$

The elements in the CP-odd Higgs mass squared matrix

$$\begin{aligned}
m_{\sigma_d \sigma_d} &= m_{H_d}^2 + |\mu|^2 + \frac{1}{8} \left( [g_1^2 + (g_X + g_{YX})^2 + g_2^2] (v_d^2 - v_u^2) \right. \\
&\quad \left. + 2(g_{YX}g_X + g_X^2)(v_\eta^2 - v_{\bar{\eta}}^2) \right) + \sqrt{2}v_S\mu\lambda_H + \frac{1}{2}(v_u^2 + v_S^2)|\lambda_H|^2,
\end{aligned}$$

$$\begin{aligned}
m_{\sigma_d \sigma_u} &= \left( (\sqrt{2} M_S v_S + l_W) + \frac{1}{2} \kappa v_S^2 + \frac{1}{2} \lambda_C v_\eta v_{\bar{\eta}} \right) \lambda_H + B_\mu + \frac{1}{\sqrt{2}} v_S T_{\lambda_H}, \\
m_{\sigma_u \sigma_u} &= m_{H_u}^2 + |\mu|^2 + \frac{1}{8} \left( [g_1^2 + (g_X + g_{YX})^2 + g_2^2] (v_u^2 - v_d^2) \right. \\
&\quad \left. + 2(g_{YX} g_X + g_X^2) (v_\eta^2 - v_{\bar{\eta}}^2) \right) + \sqrt{2} v_S \mu \lambda_H + \frac{1}{2} (v_d^2 + v_S^2) |\lambda_H|^2, \\
m_{\sigma_\eta \sigma_\eta} &= m_\eta^2 + \frac{1}{4} \left( (g_{YX} g_X + g_X^2) (v_d^2 - v_u^2) + 2g_X^2 (v_\eta^2 - v_{\bar{\eta}}^2) \right) + \frac{1}{2} (v_\eta^2 + v_S^2) |\lambda_C|^2, \\
m_{\sigma_\eta \sigma_{\bar{\eta}}} &= \frac{1}{2} \left( (-2l_W + \lambda_H v_d v_u) \lambda_C - \sqrt{2} v_S (2M_S \lambda_C + T_{\lambda_C}) - v_S^2 \lambda_C \kappa \right), \\
m_{\sigma_{\bar{\eta}} \sigma_{\bar{\eta}}} &= m_{\bar{\eta}}^2 + \frac{1}{4} \left( (g_{YX} g_X + g_X^2) (v_u^2 - v_d^2) + 2g_X^2 (v_\eta^2 - v_{\bar{\eta}}^2) \right) + \frac{1}{2} (v_\eta^2 + v_S^2) |\lambda_C|^2, \\
m_{\sigma_d \sigma_s} &= -v_u \left( (\kappa v_S + \sqrt{2} M_S) \lambda_H - \frac{1}{\sqrt{2}} T_{\lambda_H} \right), \quad m_{\sigma_d \sigma_\eta} = -\frac{1}{2} v_u v_{\bar{\eta}} \lambda_H \lambda_C, \\
m_{\sigma_u \sigma_s} &= -v_d \left( (\kappa v_S + \sqrt{2} M_S) \lambda_H - \frac{1}{\sqrt{2}} T_{\lambda_H} \right), \quad m_{\sigma_u \sigma_\eta} = -\frac{1}{2} v_d v_{\bar{\eta}} \lambda_H \lambda_C, \\
m_{\sigma_\eta \sigma_s} &= v_{\bar{\eta}} \left( (\kappa v_S + \sqrt{2} M_S) \lambda_C - \frac{1}{\sqrt{2}} T_{\lambda_C} \right), \quad m_{\sigma_d \sigma_{\bar{\eta}}} = -\frac{1}{2} v_u v_\eta \lambda_H \lambda_C, \\
m_{\sigma_{\bar{\eta}} \sigma_s} &= v_\eta \left( (\kappa v_S + \sqrt{2} M_S) \lambda_C - \frac{1}{\sqrt{2}} T_{\lambda_C} \right), \quad m_{\sigma_u \sigma_{\bar{\eta}}} = -\frac{1}{2} v_d v_\eta \lambda_H \lambda_C, \\
m_{\sigma_s \sigma_s} &= m_S^2 + 4|M_S|^2 + (\kappa v_S^2 - 2l_W - \lambda_C v_\eta v_{\bar{\eta}} + \lambda_H v_d v_u) \kappa - 2B_S \\
&\quad + \frac{1}{2} |\lambda_C|^2 \xi^2 + \frac{1}{2} |\lambda_H|^2 v^2 + \sqrt{2} v_S (2M_S \kappa - T_\kappa). \tag{54}
\end{aligned}$$

In this appendix, we collect the used vertexes, which include the couplings of:  $H - H - H$ ,  $H - W - W$  and  $H - Z - Z$

$$\begin{aligned}
\mathcal{L}_{HHH} &= iH_i H_j \left\{ \left( \frac{1}{4} g_1^2 + \frac{1}{4} g_{YX}^2 + \frac{1}{4} g_2^2 + \frac{1}{2} g_{YX} g_X + \frac{1}{4} g_X^2 - \lambda_H^2 \right) [v_u \langle 112 \rangle + v_d \langle 122 \rangle] \right. \\
&\quad \left. - \left( \frac{3}{4} g_1^2 + \frac{3}{4} g_{YX}^2 + \frac{3}{4} g_2^2 + \frac{3}{2} g_{YX} g_X + \frac{3}{4} g_X^2 \right) [v_u \langle 111 \rangle + v_d \langle 222 \rangle] + \frac{1}{2} (g_{YX} g_X + g_X^2) \right. \\
&\quad \left. \times [v_{\bar{\eta}} (\langle 114 \rangle + \langle 224 \rangle) - v_\eta (\langle 113 \rangle + \langle 223 \rangle) + v_u (\langle 233 \rangle + \langle 244 \rangle) - v_d (\langle 133 \rangle + \langle 144 \rangle)] \right. \\
&\quad \left. - (v_S \lambda_H^2 + \sqrt{2} \mu \lambda_H) (\langle 115 \rangle + \langle 225 \rangle) + (\lambda_H v_S \kappa + \sqrt{2} M_S \lambda_H + \frac{1}{\sqrt{2}} T_{\lambda_H}) \langle 125 \rangle \right. \\
&\quad \left. - (\lambda_C v_S \kappa + \sqrt{2} M_S \lambda_C + \frac{1}{\sqrt{2}} T_{\lambda_C}) \langle 345 \rangle + \frac{1}{2} \lambda_H \lambda_C [v_{\bar{\eta}} \langle 123 \rangle + v_\eta \langle 124 \rangle + v_u \langle 134 \rangle \right. \\
&\quad \left. + v_d \langle 234 \rangle] + (\lambda_H v_u \kappa - v_d \lambda_H^2) \langle 155 \rangle + (\lambda_H v_d \kappa - v_u \lambda_H^2) \langle 255 \rangle - 3g_X^2 (v_\eta \langle 333 \rangle + v_{\bar{\eta}} \langle 444 \rangle) \right. \\
&\quad \left. + (g_X^2 - \lambda_C^2) (v_\eta \langle 344 \rangle + v_{\bar{\eta}} \langle 334 \rangle) - v_S \lambda_C^2 (\langle 335 \rangle + \langle 445 \rangle) - (\lambda_C^2 v_\eta + \lambda_C v_{\bar{\eta}} \kappa) \langle 355 \rangle \right. \\
&\quad \left. - (\lambda_C^2 v_{\bar{\eta}} + \lambda_C v_\eta \kappa) \langle 455 \rangle - (6v_S \kappa^2 + 6\sqrt{2} M_S \kappa + \sqrt{2} T_\kappa) \langle 555 \rangle \right\} H_k, \\
\mathcal{L}_{HWW} &= H_i W_\mu \left( \frac{i}{2} g_2^2 (v_d Z_{i1}^H + v_u Z_{i2}^H) g^{\sigma\mu} \right) W_\sigma^*, \\
\mathcal{L}_{HZZ} &= H_i Z_\mu \left\{ \frac{i}{2} \left[ (g_1 \cos \theta'_W \sin \theta_W + g_2 \cos \theta'_W \cos \theta_W - g_{YX} g_X \sin \theta'_W)^2 \right. \right. \\
&\quad \left. \left. \times (v_d Z_{i1}^H + v_u Z_{i2}^H) + 4(g_X \sin \theta'_W)^2 (v_{\bar{\eta}} Z_{i4}^H + v_\eta Z_{i3}^H) \right] g^{\sigma\mu} \right\} Z_\sigma^*. \tag{55}
\end{aligned}$$

Here  $\langle \alpha\alpha\alpha \rangle, \langle \alpha\alpha\beta \rangle, \langle \alpha\beta\gamma \rangle$  are the shorthand notations

$$\begin{aligned}\langle \alpha\alpha\alpha \rangle &= Z_{i\alpha}^H Z_{j\alpha}^H Z_{k\alpha}^H, \quad \langle \alpha\alpha\beta \rangle = Z_{i\alpha}^H Z_{j\alpha}^H Z_{k\beta}^H + Z_{i\alpha}^H Z_{j\beta}^H Z_{k\alpha}^H + Z_{i\beta}^H Z_{j\alpha}^H Z_{k\alpha}^H, (\alpha \neq \beta), \\ \langle \alpha\beta\gamma \rangle &= Z_{i\alpha}^H Z_{j\gamma}^H Z_{k\beta}^H + Z_{i\gamma}^H Z_{j\alpha}^H Z_{k\beta}^H + Z_{i\alpha}^H Z_{j\beta}^H Z_{k\gamma}^H + Z_{i\gamma}^H Z_{j\beta}^H Z_{k\alpha}^H + Z_{i\beta}^H Z_{j\alpha}^H Z_{k\gamma}^H \\ &\quad + Z_{i\beta}^H Z_{j\gamma}^H Z_{k\alpha}^H, \quad (\alpha \neq \beta \neq \gamma).\end{aligned}\tag{56}$$

Some other used couplings are shown as

$$\begin{aligned}\mathcal{L}_{WW\tilde{\nu}^R\tilde{\nu}^R} &= \tilde{\nu}_i^R W_\nu \left( \frac{i}{2} g_2^2 \sum_{a=1}^3 Z_{ia}^{R*} Z_{ja}^{R*} g^{\mu\nu} \right) \tilde{\nu}_j^R W_\mu, \\ \mathcal{L}_{ZZ\tilde{\nu}^R\tilde{\nu}^R} &= \tilde{\nu}_i^R Z_\nu \left\{ i \sum_{a=1}^3 \left[ Z_{ia}^{R*} Z_{ja}^{R*} \left( \frac{1}{2} g_2^2 (\cos \theta_W \cos \theta'_W)^2 + \frac{1}{2} g_1^2 (\sin \theta_W \cos \theta'_W)^2 \right. \right. \right. \\ &\quad \left. \left. + g_1 g_2 \cos \theta_W \sin \theta_W (\cos \theta'_W)^2 - g_{YX} \sin \theta'_W \cos \theta'_W (g_2 \cos \theta_W + g_1 \sin \theta_W) \right. \right. \\ &\quad \left. \left. + \frac{1}{2} g_{YX}^2 (\sin \theta'_W)^2 \right) + \frac{1}{2} g_X^2 (\sin \theta'_W)^2 Z_{i3+a}^{R*} Z_{j3+a}^{R*} \right] g^{\mu\nu} \right\} \tilde{\nu}_j^R Z_\mu, \\ \mathcal{L}_{\tilde{e}\tilde{\nu}^R W} &= \tilde{e}_i \tilde{\nu}_j^{R*} \left( -\frac{i}{2} g_2 \sum_{a=1}^3 Z_{ia}^{E*} Z_{ja}^{R*} (-p_\mu^{\tilde{\nu}_j^R} + p_\mu^{\tilde{e}_i}) \right) W^\mu + h.c., \\ \mathcal{L}_{Zdd} &= \bar{d} \left[ \left( \frac{i}{6} (3g_2 \cos \theta_W \cos \theta'_W + g_1 \sin \theta_W \cos \theta'_W - g_{YX} \sin \theta'_W) \gamma_\mu P_L \right. \right. \\ &\quad \left. \left. - \frac{i}{6} (2g_1 \sin \theta_W \cos \theta'_W - (2g_{YX} + 3g_X) \sin \theta'_W) \gamma_\mu P_R \right) d \right] Z^\mu, \\ \mathcal{L}_{Z'dd} &= \bar{d} \left[ -\frac{i}{6} (3g_2 \cos \theta_W \sin \theta'_W + g_1 \sin \theta_W \sin \theta'_W + g_{YX} \cos \theta'_W) \gamma_\mu P_L \right. \\ &\quad \left. + \frac{i}{6} [2g_1 \sin \theta_W \sin \theta'_W + (2g_{YX} + 3g_X) \cos \theta'_W] \gamma_\mu P_R \right] d \right] Z'^\mu, \\ \mathcal{L}_{Zll} &= \bar{l} \left\{ \frac{i}{2} (-g_1 \sin \theta_W \cos \theta'_W + g_2 \cos \theta_W \cos \theta'_W + g_{YX} \sin \theta'_W) \gamma_\mu P_L \right. \\ &\quad \left. - \frac{i}{2} (2g_1 \sin \theta_W \cos \theta'_W - (2g_{YX} + g_X) \sin \theta'_W) \gamma_\mu P_R \right\} l Z^\mu, \\ \mathcal{L}_{Z' ll} &= \bar{l} \left\{ \frac{i}{2} (g_1 \sin \theta_W \sin \theta'_W - g_2 \cos \theta_W \sin \theta'_W + g_{YX} \cos \theta'_W) \gamma_\mu P_L \right. \\ &\quad \left. + \frac{i}{2} (2g_1 \sin \theta_W \sin \theta'_W + (2g_{YX} + g_X) \cos \theta'_W) \gamma_\mu P_R \right\} l Z'^\mu, \\ \mathcal{L}_{Zuu} &= \bar{u} \left\{ -\frac{i}{6} (3g_2 \cos \theta_W \cos \theta'_W - g_1 \sin \theta_W \cos \theta'_W + g_{YX} \sin \theta'_W) \gamma_\mu P_L \right. \\ &\quad \left. + \frac{i}{6} [-(4g_{YX} + 3g_X) \sin \theta'_W + 4g_1 \sin \theta_W \cos \theta'_W] \gamma_\mu P_R \right\} u Z^\mu, \\ \mathcal{L}_{Z' uu} &= \bar{u} \left\{ -\frac{i}{6} (-3g_2 \cos \theta_W \sin \theta'_W + g_1 \sin \theta_W \sin \theta'_W + g_{YX} \cos \theta'_W) \gamma_\mu P_L \right. \\ &\quad \left. - \frac{i}{6} [(4g_{YX} + 3g_X) \cos \theta'_W + 4g_1 \sin \theta_W \sin \theta'_W] \gamma_\mu P_R \right\} u Z'^\mu, \\ \mathcal{L}_{Z\nu\nu} &= \bar{\nu}_i \left\{ -\frac{i}{2} (g_1 \sin \theta_W \cos \theta'_W + g_2 \cos \theta_W \cos \theta'_W - g_{YX} \sin \theta'_W) \sum_{a=1}^3 U_{ja}^{V*} U_{ia}^V \gamma_\mu P_L \right. \\ &\quad \left. + \frac{i}{2} (g_1 \sin \theta_W \cos \theta'_W + g_2 \cos \theta_W \cos \theta'_W - g_{YX} \sin \theta'_W) \sum_{a=1}^3 U_{ja}^V U_{ia}^{V*} \gamma_\mu P_R \right\} \nu_j Z^\mu,\end{aligned}$$

$$\begin{aligned}
\mathcal{L}_{Z'\nu\nu} &= \bar{\nu}_i \left\{ \frac{i}{2} (g_1 \sin \theta_W \sin \theta'_W + g_2 \cos \theta_W \sin \theta'_W + g_{YX} \cos \theta'_W) \sum_{a=1}^3 U_{ja}^{V*} U_{ia}^V \gamma_\mu P_L \right. \\
&\quad \left. - \frac{i}{2} (g_1 \sin \theta_W \sin \theta'_W + g_2 \cos \theta_W \sin \theta'_W + g_{YX} \cos \theta'_W) \sum_{a=1}^3 U_{ia}^{V*} U_{ja}^V \gamma_\mu P_R \right\} \nu_j Z'^\mu, \\
\mathcal{L}_{\bar{\nu}^I \bar{\nu}^R Z} &= \bar{\nu}_i^I \bar{\nu}_j^R \left\{ \frac{1}{2} (-p_\mu^{\bar{\nu}_j^R} + p_\mu^{\bar{\nu}_i^I}) \left[ (g_1 \sin \theta_W \cos \theta'_W + g_2 \cos \theta_W \cos \theta'_W \right. \right. \\
&\quad \left. \left. - g_{YX} \sin \theta'_W) \sum_{a=1}^3 Z_{ia}^{I*} Z_{ja}^{R*} + g_X \sin \theta'_W \sum_{a=1}^3 Z_{i3+a}^{I*} Z_{j3+a}^{R*} \right] \right\} Z^\mu, \\
\mathcal{L}_{\bar{\nu}^I \bar{\nu}^R Z} &= \bar{\nu}_i^I \bar{\nu}_j^R \left\{ \frac{1}{2} (-p_\mu^{\bar{\nu}_j^R} + p_\mu^{\bar{\nu}_i^I}) \left[ - (g_1 \sin \theta_W \sin \theta'_W + g_2 \cos \theta_W \sin \theta'_W \right. \right. \\
&\quad \left. \left. + g_{YX} \cos \theta'_W) \sum_{a=1}^3 Z_{ia}^{I*} Z_{ja}^{R*} + g_X \cos \theta'_W \sum_{a=1}^3 Z_{i3+a}^{I*} Z_{j3+a}^{R*} \right] \right\} Z'^\mu, \tag{57}
\end{aligned}$$

- 
- [1] P.A.R. Ade, et al. *Astron. Astrophys.* **571**, 1054-1062 (2014); R.H. Cyburt, *Phys. Rev. D* **70**, 023505 (2004).
  - [2] G. Bertone, D. Hooper and J. Silk, *Phys. Rept.* **405**, 279-390 (2005); E. Corbelli, P. Salucci, *Mon. Not. Roy. Astron.* **311**, 441-447 (1999).
  - [3] D. Clowe, M. Bradac, A.H. Gonzalez, et al. *Astrophys. J.* **648**, 109-113 (2006).
  - [4] A. Taylor, S. Dye, T.J. Broadhurst, et al., *Astrophys. J.* **501**, 539 (1998); D. Walsh, R.F. Carswell, R.J. Weymann. *Nature*. **279**, 381-384 (1979).
  - [5] M. Drees, M.M. Nojiri, *Phys. Rev. D* **47**, 376-408 (1993); J.L. Feng, *Ann. Rev. Astron. Astrophys.*, **48**, 495-545 (2010).
  - [6] CMS Collaboration, *Phys. Lett. B* **716**, 30 (2012); ATLAS Collaboration, *Phys. Lett. B* **716**, 1 (2012).
  - [7] Particle Data Group collaboration, *Phys. Rev. D* **98**, 030001 (2018).
  - [8] S. Andreas, T. Hambye, *JCAP* **0810**, 034 (2008).
  - [9] J. Rosiek, *Phys. Rev. D* **41**, 3464 (1990)[Erratum hep-ph/9511250].
  - [10] Z. Thomas, D.T. Smith, N. Weiner, *Phys. Rev. D* **77**, 115015 (2008).
  - [11] T2K Collab., *Phys. Rev. Lett.* **107**, 041801 (2011); MINOS Collab., *Phys. Rev. Lett.* **107**, 181802 (2011).
  - [12] A. Ghosh, T. Mondal, B. Mukhopadhyaya, *Phys. Rev. D* **99**, 035018 (2019).

- [13] J.J. Cao, X.F. Guo, Y.L. He, et al., JHEP **1710**, 044 (2017); J.J. Cao, Y.L. He, L. Meng, et al., arXiv:1903.01124 [hep-ph]; J.J. Cao, X.F. Guo, Y.S. Pan, et al., arXiv:1807.03762 [hep-ph].
- [14] T. Han, H.K. Liu, S. Mukhopadhyay, et al., JHEP **1903**, 080 (2019);
- [15] B. Zhu, R. Ding, Y. Li, Phys. Rev. D **98**, 035007 (2018); J. Chang, K.M. Cheung, H. Ishida, et al., JHEP **1809**, 071 (2018); D.K. Ghosh, K. Huitu, S. Mondal, Phys. Rev. D **99**, 075014 (2019).
- [16] F. Staub, e-Print: arXiv: 0806.0538; F. Staub, Comput. Phys. Commun. **185**, 1773-1790 (2014); F. Staub, Adv. High Energy Phys. **2015**, 840780 (2015).
- [17] V. Barger, P.F. Perez, S. Spinner, Phys. Rev. Lett. **102**, 181802 (2009); P.F. Perez, S. Spinner, Phys. Lett. B **673**, 251 (2009).
- [18] P.F. Perez and S. Spinner, Phys. Rev. D **83**, 035004 (2011); J.L. Yang, T.F. Feng, Y.L. Yan, et al., Phys. Rev. D **99**, 015002 (2019).
- [19] J.L. Yang, T.F. Feng, S.M. Zhao, et al., Eur. Phys. J. C **78**, 714 (2018).
- [20] J. McDonald, Phys. Rev. D **50**, 3637-3649 (1994); G. Blanger, F. Boudjema, Comput. Phys. Commun. **192**, 322-329 (2015).
- [21] W. Chao, H.K. Guo, J. Cosmol. Astropart. Phys. **09**, 009 (2017); W. Chao, J. High Energy Phys. **04**, 034 (2017); J.J. Cao, Z.X. Heng, J.M. Yang, J.Y. Zhu, JHEP **06**, 145 (2012).
- [22] S. Gopalakrishna, A.D. Gouvea, W. Porod, JCAP **05**, 005 (2006).
- [23] X.G. He, Tong Li, Phys. Rev. D **79**, 023521 (2009).
- [24] G. Jungman, M. Kamionkowski, K. Griest, Phys. Rep. **267**, 195-373 (1996); G. Bertone, D. Hooper, J. Silk, Phys. Rep. **405**, 279-390 (2005).
- [25] S.M. Zhao, T.F. Feng, et al., Eur. Phys. J. C **78**, 324 (2018); J.J. Feng, S.M. Zhao, X.X. Dong, et al., Phys. Rev. D **99**, 095033 (2019).
- [26] M. Freytsis, Z. Ligeti, Phys. Rev. D **83**, 115009 (2011).
- [27] P. Gondolo, J. Edsjo, P. Ullio, et al., JCAP **07**, 008 (2004).